available at www.sciencedirect.com

ScienceDirect

journal homepage: www.ejconline.com

In vitro and *in vivo* suppression of hepatocellular carcinoma growth by chitosan nanoparticles

Lifeng Qi[a,c,*], *Zirong Xu*[a], *Minli Chen*[b]

[a]*Zhejiang University, Nano-biology Lab of Animal Science College, Hangzhou 310029, PR China*
[b]*Centre of Lab Animal Research, Zhejiang College of Traditional Chinese Medicine, Hangzhou 310053, PR China*
[c]*Orthopaedic Research Lab, Department of Orthopaedics, School of Medicine, West Virginia University, Morgantown 26506-9196, USA*

ARTICLE INFO

Article history:
Received 3 April 2006
Received in revised form
10 August 2006
Accepted 31 August 2006
Available online 17 October 2006

Keywords:
Hepatocellular carcinoma
Chitosan nanoparticles
Antitumour

ABSTRACT

Chitosan nanoparticles (CNP), a kind of widely used drug carrier, have shown potent cytotoxic effects on various tumour cell lines *in vitro* and *in vivo*. This study sought to evaluate the antitumour effect of CNP on growth of human hepatocellular carcinoma (BEL7402) and the possible mechanisms involved. Cells were grown in the absence and presence of various concentrations of CNP with mean particle size of about 40 nm. Cell viability, ultrastructural changes, surface charge, mitochondrial membrane potential, reactive oxygen species (ROS) generation, lipid peroxidation, DNA fragmentation and fatty acid composition were analysed by MTT assay, electron microscopy, zetasizer analysis, flow cytometry, spectrophotometric thiobarbituric (TBA) assays, DNA agarose gel electrophoresis and GC/MS respectively. For *in vivo* experiments, male BABL/c nude mice were implanted with BEL7402 cells subcutaneously to establish human hepatoma model. Chitosan, saline, and CNP with different mean particle size (40, 70 and 100 nm) were administrated by oral administration (1 mg/kg body weight). Tumour and body weight were measured, morphologic changes of tumour and liver tissues were studied under electron microscope. *In vitro*, CNP exhibited high antitumour activities with an IC_{50} value of 15.01 μg/ml, 6.19 μg/ml and 0.94 μg/ml after treatment for 24 h, 48 h and 72 h respectively. CNP could induce cell necrosis observed by electron microscope and DNA fragmentation. The antitumour mechanism was mediated by neutralisation of cell surface charge, decrease of mitochondrial membrane potential and induction of lipid peroxidation. The tumour growth inhibitory rates on BEL7402 cells in nude mice treated with chitosan and CNP with different mean particle size (40, 70 and 100 nm) were 24.07%, 61.69%, 58.98% and 34.91% respectively. Typical necrotic morphological changes of tumour tissues and no liver abnormalities were found under electron microscope. In this paper, results show a strong antitumour effect of CNP on human hepatoma cell line BEL7402 *in vitro* and *in vivo*. These findings suggest that CNP could be a kind of promising agent for further evaluations in the treatment of hepatocellular carcinoma.

1. Introduction

Hepatocellular carcinoma (HCC) is one of the most common malignancies worldwide.[1] Chemotherapy is one of the most important treatments currently available for cancer diseases. Treatment of patients with HCC remains a clinical challenge due to the disappointing effects of most chemotherapies.[2] The efficacy of chemotherapy is limited and patients have

* *Corresponding author:* Tel.: +1 304 293 1065; fax: +1 304 293 7070.
E-mail address: lifengqi01@hotmail.com (L. Qi).
0959-8049/$ - see front matter
doi:10.1016/j.ejca.2006.08.029

to suffer from serious side effects, some of which are life-threatening.[3] Therefore, progresses in developing various controlled and targeted drug delivery systems, especially on biodegradable polymer nanoparticles, have attracted more attention. Nanoparticles can provide a controlled and targeted way to deliver the encapsulated anticancer drugs and thus result in high efficacy with low side effects.[4] Doxorubicin-loaded nanoparticles were reported to show increased cytotoxicity against hepatocellular carcinoma cells *in vitro* and *in vivo*.[5]

Chitosan, the deacetylated derivative of chitin, is one of the abundant, renewable, nontoxic and biodegradable carbohydrate polymers. Chitosan has been applied broadly as a functional biopolymer in food and pharmaceutics. Chitosan is known to have various biological activities including antitumour activities, immuno-enhancing effects, antifungal and antimicrobial activities.[6,7] Chitosan nanoparticles (CNP) have been synthesised as drug carriers as reported in previous studies.[8–10] The unique character of nanoparticles due to their small size and quantum size effect could make CNP exhibit biological activities.[11] CNP with small particle size and enhanced zeta potential have been prepared and characterised in our previous reports,[11,12] and their *in vitro* and *in vivo* cytotoxic effects against various tumour cell lines were also studied. It showed that CNP with small particle size and positive surface charge could exhibit higher antitumour activity than other chitosan derivatives, and the physiochemical properties of nanoparticles such as particle size and zeta potential could make a significant effect on their antitumour activity.[13] The antitumour mechanism of CNP was related to its membrane-disrupting and apoptosis-inducing activities.[14] CNP also showed significant dose- and size-dependent antitumour activity against Sarcoma−180 and hepatoma H22 in mice.[15]

This study was undertaken to probe into the antitumour mechanism of CNP by investigating the effect on cell viability, cell morphology, DNA fragmentation, surface charge, mitochondrial membrane potential, lipid peroxidation, fatty acid composition and the *in vivo* effect of CNP on human hepatoma BEL7402 cells in nude mice.

2. Materials and methods

2.1. Drugs and chemicals

CNP with mean particle size ranging from 40 nm to 100 nm and positive surface charge about 50 mV were prepared according to the method reported in our previous studies.[11,12] CNP were formed by coacervation between positively charged chitosan (0.5%, w/v) and negatively charged sodium tripolyphosphate (0.25%, w/v). Nanoparticles with different mean size were obtained by adjusting the volume ratio of chitosan to tripolyphosphate solution. Nanoparticles were purified by centrifugation at $9000 \times g$ for 30 min. Supernatants were discarded and chitosan nanoparticles were extensively rinsed with distilled water to remove any NaOH residues, and freeze dried before further use or analysis. Chitosan nanoparticles with mean particle size about 40 nm were used for *in vitro* experiments. CNP were filtered by membrane with diameter 0.45 μm and autoclaved to remove any contaminant before use in cell culture. The obtained nanoparticles were stable under the autoclaving conditions.[11] Trypsin and rhodamine 123 were purchased from Sigma Chemicals (St. Louis, MO, USA).

2.2. Cell culture conditions

BEL7402 cells were obtained from the Cell Bank of the Chinese Academy of Science, Shanghai, China. The cell line was cultured in RPMI−1640 (Gibco, Life Technologies, Vienna, Austria) supplemented with 10% heat-inactivated foetal bovine serum (Gibco) and 100 U/ml penicillin+0.1 mg/ml streptomycin in 75 cm^2 tissue plastic flasks (Corning, USA). Cells were maintained at 37 °C in a humidified 5% CO_2 atmosphere and maintained in a log-phase-growth at about $3–6 \times 10^5$ cells/ml.

2.3. Cell viability assay

Before use, BEL7402 cells were digested by 0.25% trypsin, collected and the cell number counted, then diluted into cell suspension at a density of 1×10^5/ml in complete medium, and seeded into 96-well plates at 200 μl/well. After being cultured for 24 h, the cells were immediately treated with various doses (25, 50, 75, 100 μg/ml) of CNP for another 24, 48, and 72 h. The effect of different treatments on cell viability was assessed by the tetrazolium dye (MTT) assay.[16] Control cells were also cultured at the same time. Cell proliferation and inhibition curves were drawn, and the inhibitory concentration against 50% cells (IC_{50}) was determined.

2.4. Ultrastructural cell morphology

BEL7402 cells grown on glass coverslips were incubated with 25 μg/ml CNP for 4 h. The appropriate solvent was added to the control. CNP-treated and untreated cells were fixed in glutaraldehyde/paraformaldehyde solution and prepared for scanning electron microscopy (SEM) by the triple-fixation GTGO methods.[14] The surface morphology of cells was examined by a XL30-ESEM scanning electron microscope.

BEL7402 cells grown on glass coverslips were incubated with 25 μg/ml CNP for 24 h. 0.1 M PBS was added to the controls. CNP-treated and untreated cells were fixed in glutaraldehyde/paraformaldehyde solution and prepared for transmission electron microscopy (TEM) as previously described.[14] Observations and micrographs were made under a JEM-1200EX transmission electron microscope.

2.5. DNA fragmentation

After treatment with 25 μg/ml CNP for 1 h and 4 h, BEL7402 cells were collected and DNA was extracted according to previous methods.[14] The DNA samples thus obtained were run on a 1.5% agarose gel at 50 V and visualised by ethidium bromide staining under UV light.

2.6. Changes in surface potential of cells

Zeta potential is defined as the difference in electrical potential between the surface of the cells and the bulk surrounding medium.[17] It is a measure of the net distribution of electrical charge on the surface of the cells. In this paper,

the changes in zeta potential of BEL7402 cells treated with CNP for different time were determined as followed. BEL7402 cells grown on glass coverslips were incubated with 25 μg/ml CNP at intervals from 30 min to 4 h. The cells were detached by adding 0.25% trypsin solution to prepare cell suspension. Then the surface potential of cell suspension was determined using Zetasizer Nano-ZS90 (Malvern Instruments). The analysis was performed at a scattering angle of 90° at 25 °C using samples diluted to different concentrations with de-ionised water.

2.7. Determination of mitochondrial membrane potential

To study mitochondrial membrane potential (MMP), the cells were treated with 25 μg/ml CNP at different intervals from 30 min to 4 h respectively, and then stained with 10 μg/ml rhodamine 123 which is easily sequestered by the mitochondrial membrane.[18] Once the mitochondrial membrane potential is lost, rhodamine 123 is subsequently washed out of the cells. The mitochondrial membrane potential was determined using FACSCalibur flow cytometer (Becton Dickinson, San Jose, CA) and analysed by a Cell Quest software program (BD PharMingen, FRANKLIN Lakes, USA).

2.8. Determination of reactive oxygen species and lipid peroxidation

The cells treated with various doses (25, 50, 75, 100 μg/ml) of CNP for 24 h were harvested, washed twice and resuspended in Hank's buffered saline solution (HBSS). Reactive oxygen species (ROS) production was studied by measuring the fluorescence intensity of dichlorofluorescein (DCF) as described by Buyukavci and colleagues.[19] Non-fluorescent 2,7-dichlorofluorescin-diacetate (DCFH-DA) diffuses into the cell through the plasma membrane and is hydrolysed within the cell to DCFH. Intracellular oxidation converts DCFH into the fluorescent form, DCF. DCFH-DA (Molecular Probes, Eugene, OR, USA) was stored under liquid nitrogen vapour as a 1 mM stock solution in ethanol. Cells were washed with PBS and incubated in 1 ml of DMEM with 5 μM DCFH-DA (1:200 dilution) for 60 min. Samples were analysed using FACSCalibur flow cytometer (Becton Dickinson, San Jose, CA). Fluorescence intensity was calculated as percent increase of fluorescence intensity when compared with the control sample [(fluorescence intensity of cells in treated sample/fluorescence intensity of cells in the control sample)×100].

Lipid peroxidation products were measured by the spectrophotometric thiobarbituric (TBA, Sigma, MO, USA) assays as described by Hofmanova and colleagues.[20] Briefly: 0.75 ml of cell suspension treated with various doses of CNP for 24 h was added to the TBA reagent (0.5 ml of 15% trichloroacetic acid; 0.5 ml of 0.25 N hydrochloric acid; 0.5 ml of 0.6% TBA). This mixture was incubated at 90 °C for 45 min, then cooled, extracted with 2.25 ml of N-butanol, and centrifuged (5 min, 1500 g). The absorbance of the upper phase was measured at 532 nm. The concentration of thiobarbituric acid reactive substances (TBARs) was calculated from a standard calibration curve generated with known amounts of 1,1,3,3-tetraethoxypropane (Sigma, MO, USA).

2.9. Fatty acid analysis

The fatty acid composition of BEL7402 cell membrane was determined after the cells were treated with 25 μg/ml CNP for 4 h. The total lipids were extracted from the cells by using the procedure of Bligh and Dyer.[21] The lipid extract was dried down under nitrogen and was saponified by incubation at 65 °C for 30 min to release the free fatty acids. Following acidification with hydrochloric acid, the free fatty acids were taken up into benzene. Fatty acid methyl esters (FAME) were prepared by using the method of Morrison and Smith.[22] Unwanted salts were taken up and removed with distilled water, the FAME were dried down and dissolved in trimehylpentane, and then analysed by GC/MS (HP6890GC/5973MsM, USA).

2.10. Antitumour activity in vivo

Male athymic BALB/c nude mice, 5-weeks-old weighing 15–25 g at the start of the study, were used. Human hepatoma cells (BEL7402, about 5×10^6 per 0.2 ml) were implanted subcutaneously into right flank of the nude mice. Four days after inoculation, when the tumour volumes reached $2 \times 2 \times 2$ mm^3, animals were randomly assigned to five treatment groups (n = 10 per group). Each treatment group received respective 1 mg/kg once daily chitosan or CNP with different particle size (40, 70, 100 nm) dissolved in physiological saline by oral administration (p.o.), while 0.9% saline was provided for the control group. Positive control group of cisplatin (cDDP) was administered intravenously (0.75 mg/kg body weight). Mice were allowed food and water ad libitum for up to 4 weeks. The animals were sacrificed, and the tumours were dissected and weighed. Inhibition ratio was calculated by following formula: inhibition ratio (%) = $[(A–B)/B] \times 100$, where A is average tumour weight of the negative control group, and B is that of the treatment group. All experiments were carried out according to the guidelines of the local Ethics Committee for Animal Use.

Tumour and liver specimens were prefixed in 25 g/L glutaraldehyde, then in 10 g/L OsO4, dehydrated in ethanol series, and replaced in propene oxide.[23] The samples were examined with a JEM-1200EX transmission electron microscope.

2.11. Statistical analyses

Results are presented as mean±SD. The 2-way ANOVA and Student's t test were used to compare data from different treatment groups. When P was less than 0.05, differences were considered significant.

3. Results

3.1. Inhibitory effect on proliferation of BEL7402 cells

Fig. 1 shows the cell viability curve at various concentrations of CNP. The inhibition of cell viability of BEL7402 cells by CNP was clearly observed in a dose- and time-dependent manner. The median lethal concentration of CNP was 15.01 μg/ml, 6.19 μg/ml and 0.94 μg/ml for BEL7402 at 24 h, 48 h and 72 h respectively.

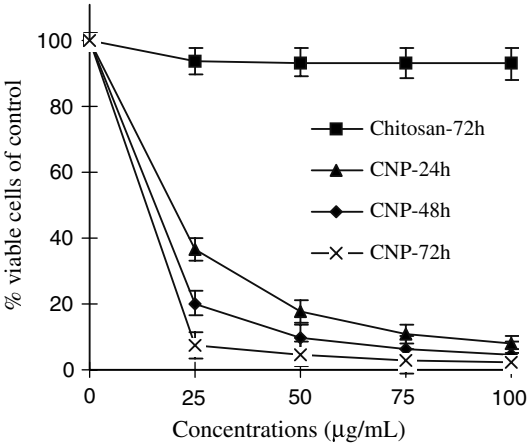

Fig. 1 – Effect of CNP on the viability of hepatoma BEL7402 cells incubated in the presence of increasing concentrations of CNP for 24 h, 48 h and 72 h *in vitro*.

3.2. *Necrotic cell morphology*

The ultrastructural alterations of BEL7402 cells treated with CNP were observed under scanning electron microscope and transmission electron microscope. Similar results as our previous report were obtained. The control cell surface showed the presence of numerous randomly distributed microvilli. After 4 h treatment with CNP, the cells broke into honeycomb shape-like pieces, necrotic cell death as evidenced by an early loss of membrane integrity, pore forming surface morphology was observed, and examined by SEM observations (Fig. 2). The completely disruption of cell membrane, dispersed chromatin fragments, vacuolated cytoplasm and organelles were also revealed under TEM (Fig. 3). The necrotic cell morphology indicated the unique penetrating mode of CNP against BEL7402 cells.

3.3. *DNA fragmentation*

DNA was extracted from cultured BEL7402 cells treated with 25 μg/ml CNP for 1 h and 4 h, the occurrence of necrosis was detected by agarose gel electrophoresis. Specific DNA degradative smearing typical of necrotic degeneration[24] was prominent in cells incubated with CNP for 1 h, and the fragmented DNA increased greatly in cells treated for 4 h (Fig. 4). It showed that CNP mainly induce the necrotic cell death resulting from the disruption of cell membrane at early treatment.

3.3.1. *Alterations of surface potential and mitochondrial membrane potential (MMP)*

In this study, CNP caused a time-dependent decrease of negative surface potential and MMP in BEL7402 cells treated with 25 μg/ml CNP at different intervals from 30 min to 4 h (Fig. 5). After 4 h of treatment, the zeta potential of cells fell to −0.92 mV from the −9.39 mV of non-treated cells. It showed that CNP could neutralise the negative surface charge of BEL7402 cells so as to damage the cell membrane.

The percentage of cells with the loss of mitochondrial membrane potential increased significantly with the increase of treatment time, and reached 39% when treated for 4 h

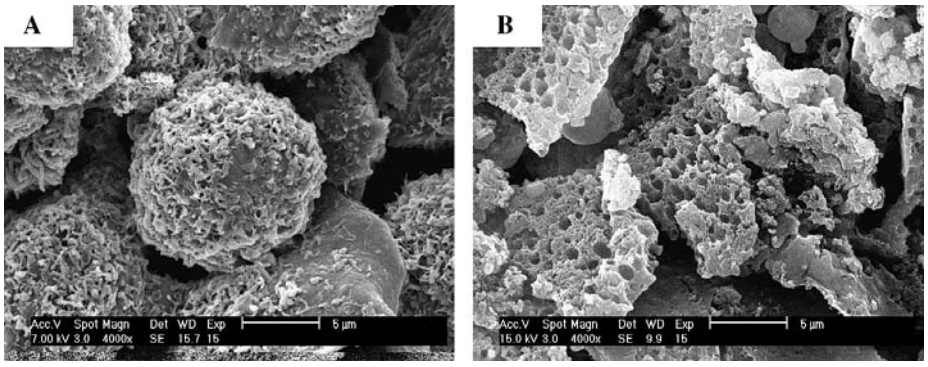

Fig. 2 – SEM photographs (the bar is 5 μm) of BEL7402 cells before (A) and after (B) 25 μg/ml CNP treatment for 4 h.

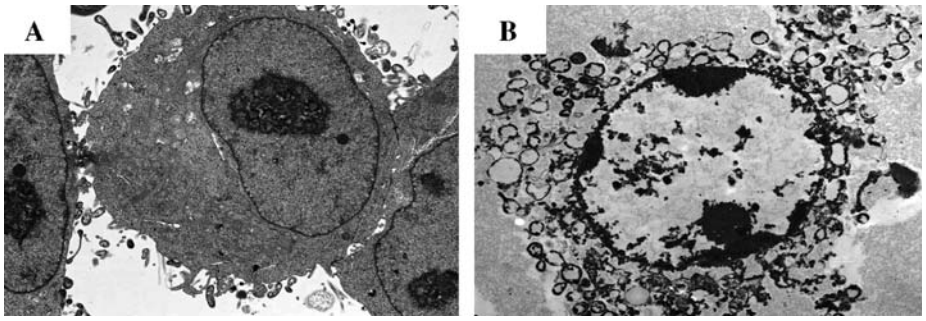

Fig. 3 – TEM photographs of BEL7402 cells before (A) and after (B) 25 μg/ml CNP treatment for 24 h (×5000).

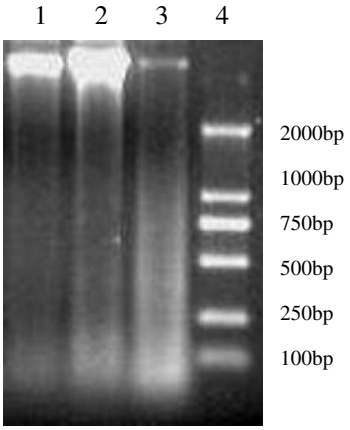

Fig. 4 – Agarose gel electrophoretic analysis of DNA isolated from BEL7402 cells incubated with 25 μg/ml CNP for 1 h (lane 2) and 4 h (lane3) or without treatment (lane 1). Lane 4: a DNA marker.

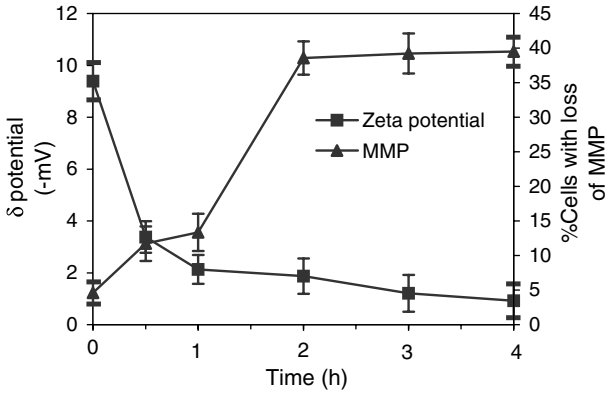

Fig. 5 – Time course changes of zeta potential and mitochondrial membrane potential (MMP) induced by CNP. The negative zeta potential of cells and the percentage of cells with the loss of MMP were drawn.

(Fig. 5). The strong dissipation in MMP suggests a possible disruption of mitochondrial membrane when cells treated with CNP.[14]

3.4. *Effects of CNP on lipid peroxidation*

Membrane lipid peroxidation was studied at the end of 24 h incubation. In cells treated with various doses of CNP, dose-dependent increase of ROS generation (DCF fluorescence intensity) and lipid peroxidation (TBARs production) were observed. DCF fluorescence intensity of cells treated with 25 μg/ml CNP was twofold higher than control samples. When 100 μg/ml CNP were used in cells, ROS generation increased about sixfold higher than control (Fig. 6). The TBARs production also increased significantly with the increase of CNP concentration. The TBARs level produced in cells reached about 1.2 nmol/million cells after treated with 100 μg/ml CNP (Fig. 7). The results showed that CNP could lead to the lipid peroxidation of cell membrane.

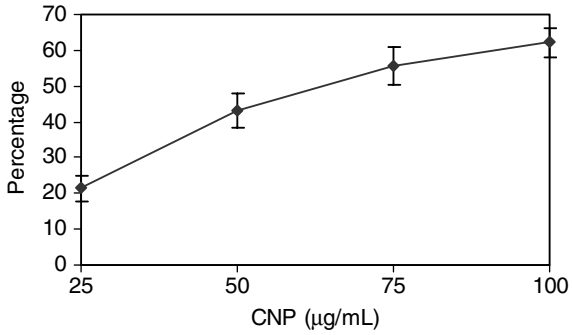

Fig. 6 – Flow cytometric analysis of ROS production (DCF:10*) with various doses of CNP treatment for 24 h. (*) % increase of DCF fluorescence intensity versus control group.

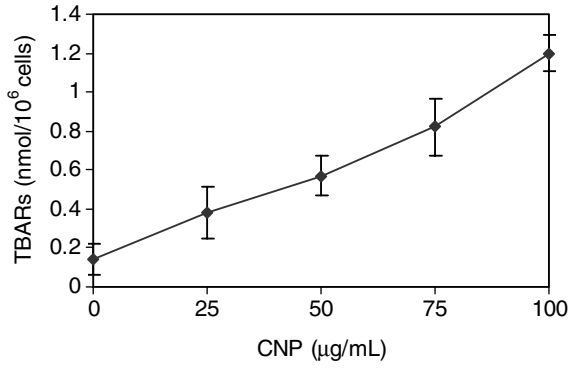

Fig. 7 – Lipid peroxidation measured as thiobarbituric acid reactive substances (TBARs) production of BEL7402 cells non-treated or treated for 24 h with various doses of CNP.

3.4.1. *Changes in lipid composition induced by CNP*

The antitumour activities of CNP have been related with the membrane permeabilising capability of the nanoparticles in our previous report.[14] Therefore, to explore the possibility of membrane pore forming function of CNP, the effect on the lipid composition was examined. Table 1 presents changes in the amount of each lipid class upon CNP treatment. After treatment with 25 μg/ml CNP for 24 h, the content of unsaturated fatty acid of cell membrane decreased greatly. The ratios for decrease of C18:1, C18:2, and C20:4 were 24.6%, 12.4% and 24% respectively. The changes in the lipid composition induced by CNP were probably consequences of membrane permeabilisation brought about by the membrane perturbing action of nanoparticles.

Table 1 – Effects of CNP on fatty acid composition of membrane phosphoric lipid

Fatty acid	Control (μg/mg)	CNP treatment (μg/mg)
$C_{14:0}$	29.93 ± 2.01	30.29 ± 2.21
$C_{16:0}$	216.5 ± 13.73	215.51 ± 5.41
$C_{18:0}$	255.61 ± 14.86	252.11 ± 10.99
$C_{18:1}$	142.62 ± 8.52	108.66 ± 5.11[a]
$C_{18:2}$	226.22 ± 8.29	195.78 ± 4.54[a]
$C_{20:4}$	12.97 ± 1.46	9.87 ± 0.45[a]

a $P < 0.01$ *versus* control.

Table 2 – Effect of CNP with different particle size on BEL7402 tumour cell growth in nude mice by oral administration (1 mg/kg/day)

Sample	Increase of body weight (g)	Tumour weight (g)	Inhibition (%)
Control	1.54 ± 0.56	2.95 ± 0.46	–
cDDP	−2.3 ± 0.99	0.56 ± 0.13	80.9
Chitosan	1.78 ± 0.97	2.24 ± 0.41	24.07
CNP (40 nm)	2.40 ± 0.44	1.13 ± 0.22	61.69
CNP (70 nm)	2.38 ± 0.48	1.21 ± 0.29	58.98
CNP (100 nm)	1.96 ± 0.85	1.92 ± 0.46	34.91

3.5. *Effect of CNP on tumour growth in vivo*

The results in Table 2 showed that CNP with different particle size (40, 70, 100 nm) exhibited an antitumour effect against BEL7402 cells when administrated by oral administration (p.o.). The inhibition rate respectively reached 61.69%, 58.98% and 34.91% at a low dose of 1 mg/kg/day, much higher than the antitumour activity of chitosan group as 24.07%. cDDP as positive control drug exhibited higher antitumour efficacy than CNP. However, cisplatin also showed great side effects compared with CNP. CNP resulted in a great increase in body weight of the mice relative to the saline control, which indicated few side effects. On the contrary, cDDP led to a significant lose in body weight of mice. Otherwise, cDDP also had a lethal toxicity as 2/10, while in chitosan and CNP groups, no lethal toxicity occurred for the inhibition of tumour growth.

3.6. *Pathological observation of tumour and liver tissues*

The morphologic changes of tumour tissues were observed by TEM (Fig. 8). Large areas of necrosis such as disruption of the cytoplasm and appearance of remnants of swollen organelles

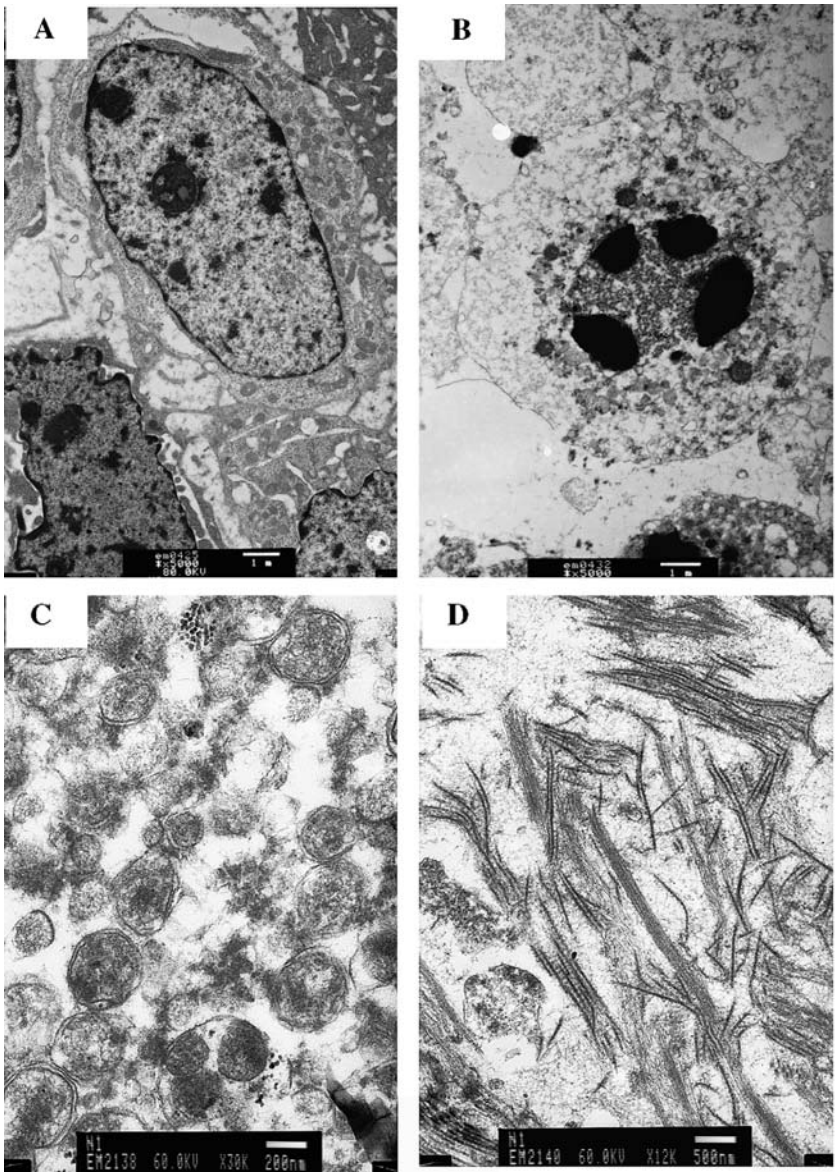

Fig. 8 – TEM photographs of tumour tissues after CNP oral administration. (A): Control ×5000; (B): CNP group ×5000; (C): CNP group ×30,000; (D): CNP group ×12,000.

were seen in CNP administrated group under electron microscope. In saline group of mice, BEL7402 cells in areas of non-necrosis proliferated rapidly and cells showed integral membrane distributed with microvilli and normal organelle. While in CNP groups, the cells became vacuolated, the plasma membrane and nuclear envelope were disrupted completely, the mitochondrion was swollen, the chromatin was condensed and disorganised, the nuclei were distorted greatly, and fibrosis was also seen. In chitosan group, only a few areas of necrosis were seen due to the lower inhibitory rate.

Liver histopathology was studied to evaluate the cytotoxic effect of CNP against normal tissues by TEM observation. It showed that liver tissues of CNP-treated mice exhibited more normal ultrastructural morphology compared with positive control (cDDP) group. In cDDP group, liver abnormalities were observed due to the cytotoxic effects of cDDP on hepatocytes, histopathological findings in the liver tissue were characterised by extensive damage and minor necrotic foci (Fig. 9). Condensed nucleus, particularly dissolution and partial agglomeration of chromatin, swollen mitochondria, fatty degeneration of liver cells and slight dissolution of organelles were observed. While in the groups treated with CNP, liver cells showed much better morphology. Ultrastructure turns normal, cytoplasm and organelles such as mitochondria showed more clearly, and little fatty vesicles were found. Therefore, CNP exhibited fewer side effects against normal cells compared with cDDP.

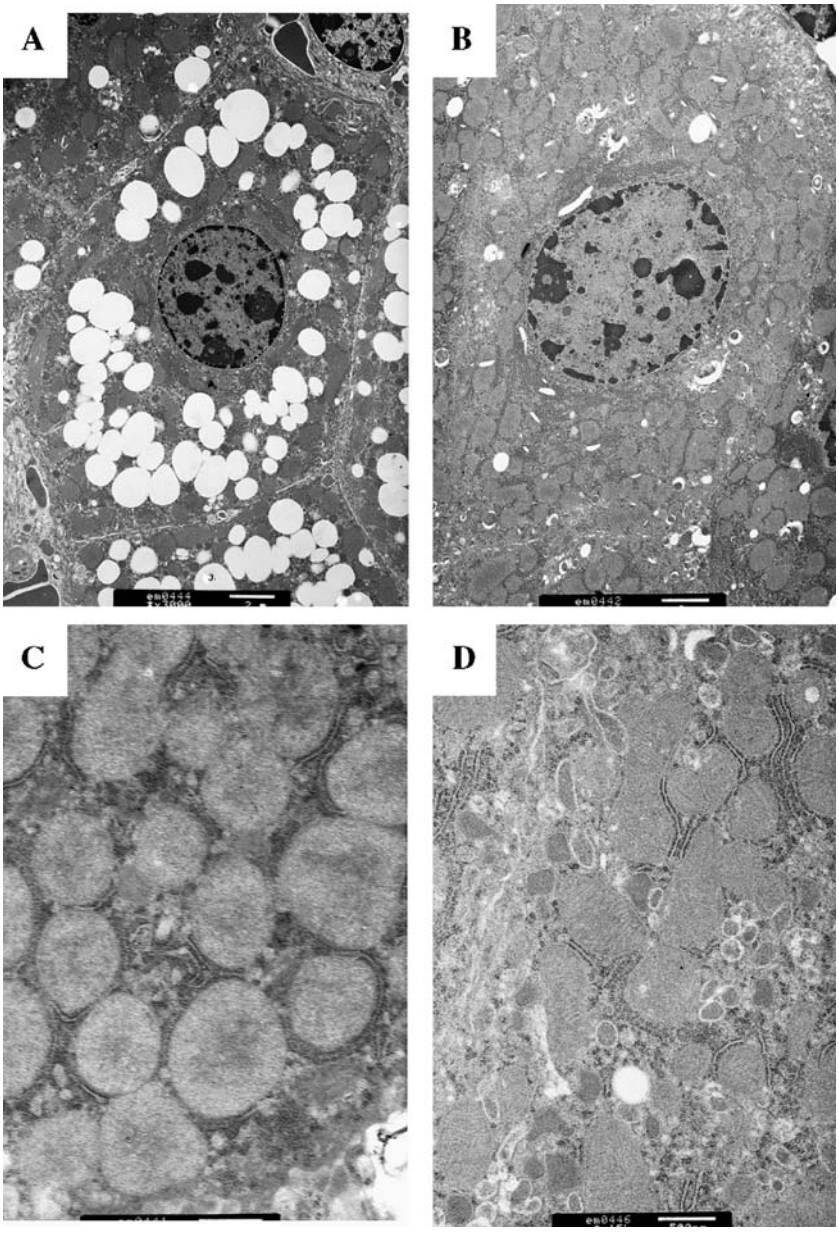

Fig. 9 – TEM photographs of liver tissue from nude mice before and after CNP administration. (A): cDDP group ×3000; (B): CNP group ×3000; (C): cDDP group ×15,000; (D): CNP group ×15,000.

4. Discussion

Cancer diseases especially human hepatocellular carcinomas are the leading causes for deaths. Chemotherapy is one of the most important treatments applied broadly for cancer diseases. The present status of chemotherapy is far from being satisfactory. The efficacy of chemotherapy is limited due to the serious side effects and drug resistance.[3] Various targeted drug delivery systems especially on polymer nanoparticles have been developed in recent years, these nanoparticles have a size small enough to allow intracapillary or transcapillary passage and appropriate surface coating to escape from macrophage uptake and overcome the drug resistance problem, thus greatly improving the efficacy of drugs and decreasing the side effects.[25–27] Positively charged chitosan nanoparticles (CNP) targeting cancer cell membrane have been developed by our laboratory. CNP exhibited high antitumour activity against various tumour cell lines by induction of necrotic cell death.[13–15] In this study, the *in vitro* and *in vivo* effects of CNP on human hepatoma BEL7402 cells were investigated.

CNP demonstrated a strong antitumour activity *in vitro* by reducing cell viability, inducing cell necrosis, decreasing the negative surface charge and mitochondrial membrane potential, induction of lipid peroxidation, disturbing the fatty acid composition of membrane and fragmenting DNA. After treatment for 72 h, almost no viable cells were detected. CNP elicited dose-dependent and time-dependent inhibitory effects on the proliferation of tumour cell lines, while chitosan didn't show effective activity when its concentration reached 100 μg/ml. CNP with different particle size exhibited targeted cytotoxic activities against hepatoma BEL7402 cells while no effects on normal liver cells, the little particle size and high surface charge of CNP are responsible for their high cytotoxicity.[13]

CNP could induce mostly necrotic cell death of human gastric cancer cells by disrupting cell membrane.[14] Cell death mechanisms could be distinguished by morphological criteria under electron microscope.[28] The morphological changes that characterise apoptosis are mainly cell shrinkage and rounding with initially intact plasma membrane. While the morphology of necrotic cells was characterised as appearance of bubbles, loss of the plasma membrane integrity, uniform chromatin condensation and dispersion. In this study, the CNP-treated cells exhibited typical necrotic morphology as described above and DNA fragment specific for necrosis, this showed that CNP mainly induced cell necrosis by disrupting membrane.

Cancer cells exhibit relatively low resting membrane potentials compared with normal proliferating cells.[29] Even rather small changes in surface potential could cause a proportionally large change in the transmembrane electric field.[30] In this study, CNP could induce a positive shift of cell surface potential, which indicated that surface charge neutralisation was the first step of interaction between nanoparticles and cell membrane. Positive shift of surface charge and the significant decrease of mitochondrial membrane potential revealed the membrane perturbing activity of CNP, because decrease of mitochondrial membrane potential (MMP) was related with mitochondrial membrane damage and loss of cell membrane integrity.[14]

Increased reactive oxygen species (ROS) production and lipid peroxidation (LPO) also played a role in cell death induced by CNP. ROS, which are continuously produced in cells, can stimulate LPO. ROS cause nonspecific damage to lipids, proteins, and DNA, leading to alteration or loss of cellular function. Many studies have associated mitochondrial dysfunction caused by ROS with both necrotic and apoptotic cell death.[31] LPO is commonly regarded as a deleterious mechanism, leading to structural modification of complex lipid protein assemblies, such as biomembranes, and is usually associated with cellular dysfunction.[32] In this study, the mitochondrial membrane damage indicated by loss of MMP could be attributed to the increased ROS production and lipid peroxidation, which led to the necrotic cell death.

Fatty acids, especially those in ester phospholipids, control the structure and function of biological membranes by influencing membrane fluidity.[33] Membrane perturbation by an amphiphilic peptide, Mastoparan 7 was related with a broad alteration in lipid composition.[34] The pore forming activity of CNP in cancer cells had been observed by SEM previously[14] and was confirmed in this study. It is well known that the unsaturated fatty acids are substrates of lipid peroxidation (LPO) and their level before and after induction testifies to the LPO degree. Lipid peroxidation with decrease of unsaturated fatty acids had been inducted by ultrasonication in Ehrlich ascetic tumour cells[35] Increased ROS production and LPO degree after CNP treatment were observed in this study. The significant decrease in unsaturated fatty acid indicated that CNP exerted membrane perturbation activity by induction of LPO.

The *in vivo* antitumour effect of CNP against BEL7402 cells was investigated in the present study. CNP with different particle size by oral administration (p.o.) showed greatly increased cytotoxic efficacy than chitosan against hepatoma BEL7402 cells in nude mice. We observed the morphologic changes of necrosis by TEM in CNP group, the tumour cell membrane and cytoplasm were disrupted completely, swollen organelles and fibrosis were observed. There was a higher inhibitory rate of tumour in cDDP group, but the weight of nude mice was reduced greatly and a lethal toxicity as 2/10 was shown due to its side effects. Liver abnormalities were also observed due to the cytotoxic effects of cDDP on hepatocytes. While for CNP group, few side effects were observed. Body weights of mice increased and the morphology of liver tissues turned normally.

Oral delivery of anticancer drugs can provide a long-time, continuous exposure of cancer cells to the drugs of a relatively lower thus safer concentration and thus give little chance for the tumour blood vessels to grow, resulting in much better efficacy and fewer side effects than the current regime of drugs by injection or infusion.[36] It has been found that the size of the nanoparticles plays a key role in their interaction with the biological cells and the *in vivo* fate of a particulate drug delivery system.[37,38] The smaller size particles seem to have efficient interfacial interaction with the cell membrane compared to larger size particles, thus improving efficacy of the particle-based oral drug delivery systems. The use of particle size reduction to increase the oral bioavailability of drugs has been obtained.[39] In the present study, the

tumour inhibitory rate increased with the decrease of mean particle size of CNP.

Zeta potential of nanoparticles is also an important factor to determine their interaction *in vivo* with the tumour cell membrane, which is usually negatively charged.[40] Enhancement of electrostatic interaction between the mucosal surfaces and drugs have a marked effect on their uptake and overall bioavailability, since the epithelial cells in the various tissues including gastrointestinal tract, carry a negative surface charge.[41] Positively charged colloidal drug carriers could increase the permeability and overall bioavailability of the drugs while reducing their side effects, which was due to the mucoadhesion mediated by electrostatic interaction between the positively charged colloidal particles and the negatively charged mucin on the mucosal surface.[42] CNP used in the study exhibit a high surface charge with 52 mV much higher than that of chitosan as determined previously.[14] Therefore, the higher *in vivo* antitumour activity of CNP is partly due to its high surface charge.

In summary, CNP with little particle size and high surface charge exhibited a strong dose- and time-dependent antitumour activity on human hepatoma BEL7402 cells *in vitro*, and could induce cell necrosis by neutralising surface charge, permeating cell membrane, decreasing MMP and inducing lipid peroxidation. CNP showed higher tumour inhibitory effects than chitosan *in vivo*, particle size of CNP could make a great effect on its antitumour activity. Therefore, CNP could be a potent agent in the treatment of hepatocellular carcinoma for further evaluations.

Conflict of interest statement

None declared.

REFERENCES

1. de Jough FE, Janssen HL, de Man RA, Hop WC, Schalm SW, van Blankenstein M. Survival and prognostic indicators in hepatitis B surface antigen-positive cirrhosis of the liver. *Gastroenterology* 1992;**103**:1630–5.
2. Bruix J. Treatment of hepatocellular carcinoma. *Hepatology* 1997;**25**:259–62.
3. Feng SS, Chien S. Chemotherapeutic engineering: Application and further development of chemical engineering principles for chemotherapy of cancer and other diseases. *Chem Eng Sci* 2003;**58**:4087–114.
4. Langer R. Biomaterials in drug delivery and tissue engineering: One laboratory's experience. *Accounts Chem Res* 2000;**33**:94–101.
5. Barraud L, Merle P, Soma E, et al. Increase of doxorubicin sensitivity by doxorubicin-loading into nanoparticles for hepatocellular carcinoma cells in vitro and in vivo. *J Hepatol* 2005;**42**:629–31.
6. Sudarshan NR, Hoover DG, Knorr D. Antibacterial action of chitosan. *Food Biotechnol* 1992;**6**:257–72.
7. Tsai GJ, Su WH. Antibacterial activity of shrimp chitosan against Escherichia coli. *J Food Prot* 1999;**62**:239–43.
8. Janes KA, Fresneau MP, Marazuela A, Fabra A, Alonso MJ. Chitosan nanoparticles as delivery systems for doxorubicin. *J Control Rel* 2001;**73**:255–67.
9. De Campos AM, Sanchez A, Alonso MJ. Chitosan nanoparticles: a new vehicle for the improvement of the delivery of drugs to the ocular surface. Application to cyclosorin A. *Int J Pharm* 2001;**224**:159–68.
10. Xu Y, Du Y. Effect of molecular structure of chitosan on protein delivery properties of chitosan nanoparticles. *Int J Pharm* 2003;**250**:215–26.
11. Qi L, Xu Z, Jiang X, Hu C, Zou X. Preparation and antibacterial activity of chitosan nanoparticles. *Carbohyd Res* 2004;**339**:2693–700.
12. Qi L, Xu Z. Lead sorption from aqueous solutions on chitosan nanoparticles. *Colloid Surface A* 2004;**251**:183–90.
13. Qi L, Xu Z, Jiang X, Li Y, Wang M. Cytotoxic activities of chitosan nanoparticles and copper-loaded nanoparticles. *Bioorg Med Chem Lett* 2005;**15**:1397–9.
14. Qi L, Xu Z, Li Y, Jiang X, Han X. In vitro effects of chitosan nanoparticles on growth of human gastric cancer cell line MGC803 cells. *World J Gastroentero* 2005;**11**:5136–41.
15. Qi L, Xu Z. In vivo antitumour activity of chitosan nanoparticles. *Bioorg Med Chem Lett* 2006;**16**:4243–5.
16. Truter EJ, Santos AS, Els WJ. Assessment of the antitumour activity of targeted immunospecific albumin microspheres loaded with cisplatin and 5-fluorouracil: toxicity against a rodent ovarian carcinoma in vitro. *Cell Biol Int* 2001;**25**:51–9.
17. McLaughlin S. The electrostatic properties of membranes. *Ann Rev Biophys Biophys Chem* 1989;**18**:113–36.
18. Kim H, You S, Kong BW, Foster LK, Farris J, Foster DN. Necrotic cell death by hydrogen peroxide in immortal DF-1 chicken embryo fibroblast cells expressing deregulated MnSOD and catalase. *Biochim Bioph Acta* 2001;**1540**:137–46.
19. Buyukavci M, Ozdemir O, Buck S, Stout M, Ravindranath Y, Savasan S. Melatonin cytotoxicity in human leukemia cells: relation with its pro-oxidant effect. *Fundam Clin Pharmacol* 2006;**20**:73–9.
20. Hofmanova J, Vaculova A, Lojek A, Kozubik A. Interaction of polyunsaturated fatty acids and sodium butyrate during apoptosis in HT-29 human colon adenocarcinoma cells. *Eur J Nutr* 2005;**44**:40–51.
21. Bligh EG, Dyer WJ. A rapid method for total lipid extraction and purification. *Can J Biochem Physiol* 1959;**37**:911–7.
22. Morrison WR, Smith LM. Preparation of fatty acid methyl esters and dimethylacetals from lipids with boron fluride-methanol. *J Lipid Res* 1964;**5**:600–8.
23. Xu HY, Yang YL, Liu SM, Bi L, Chen SX. Effect of arsenic trioxide on human hepatocarcinoma in nude mice. *World J Gastroentero* 2004;**10**:3677–9.
24. Kok YJ, Swe M, Sit KH. Necrosis has orderly DNA fragmentations. *Biochem Bioph Res Co* 2002;**294**:934–9.
25. Ahsan F, Rivas IP, Khan MA, Torres Suarez AI. Targeting to macrophages: Role of physicochemical properties of particulate carriers-liposomes and microspheres-on the phagocytosis by macrophages. *J Control Release* 2002;**79**:29–40.
26. Dellacherie E, Gref R, Quellec PS. Nanospheres as new injectable drug carriers: A promising way? *MS-Medicine Sci* 2001;**17**:619–26.
27. Johnson OL, Cleland JL, Lee HJ, et al. A month-long effect from a single injection of microencapsulated human growth hormone. *Nat Med* 1996;**3**:795–9.
28. Rello S, Stockert JC, Moreno V, et al. Morphological criteria to distinguish cell death induced by apoptotic and necrotic treatments. *Apoptosis* 2005;**10**:201–8.
29. Binggeli R, Weinstein RC. Membrane potentials and sodium channels: hypotheses for growth regulation and cancer formation based on changes in sodium channels and gap junctions. *J Theor Biol* 1986;**123**:377–401.

30. Annarosa A, Carla M, Del Bene M, Becchetti A, Wanke E, Olivotto M. Polar/apolar compounds induce leukemia cell differentiation by modulating cell-surface potential. *Proc Natl Acad Sci USA* 1993;**90**:5858–62.
31. Zhao K, Zhao GM, Wu D, et al. Cell-permeable peptide antioxidants targeted to inner mitochondrial membrane inhibit mitochondrial swelling, oxidative cell death, and reperfusion injury. *J Biol Chem* 2004;**279**:34682–90.
32. Maheo K, Vibet S, Steghens JP, et al. Differential sensitization of cancer cells to doxorubicin by DHA: a role for lipoperoxidation. *Free Radic Biol Med* 2005;**39**:742–51.
33. Heude B, Ducimetiere P, Berr C. Cognitive decline and fatty acid composition of erythrocyte membranes-The EVA Study. *Am J Clin Nutr* 2003;**77**:803–8.
34. Park HS, Lee SY, Kim YH, Kim JY, Lee SJ, Choi M. Membrane perturbation by mastoparan 7 elicits a broad alteration in lipid composition of L1210 cells. *Biochim Biophys Acta* 2000;**1484**:151–62.
35. Hristov PK, Petrov LA, Russanov EM. Lipid peroxidation induced by ultrasonication in Ehrlich ascetic tumour cells. *Cancer Lett* 1997;**121**:7–10.
36. Win KY, Feng SS. Effects of particle size and surface coating on cellular uptake of polymeric nanoparticles for oral delivery of anticancer drugs. *Biomaterials* 2005;**26**:2713–22.
37. Foster KA, Yazdanian M, Audus KL. Microparticulate uptake mechanisms of in-vitro cell culture models of the respiratory epithelium. *J Pharm Pharmacol* 2001;**53**:57–66.
38. Moghimi SM, Hunter AC, Murray JC. Long-circulating and target-specific nanoparticles: Theory to practice. *Pharmacol Rev* 2001;**53**:283–318.
39. Gary GL, Kenneth CC. Particle size reduction for improvement of oral bioavailability of hydrophobic drugs: I. Absolute oral bioavailability of nanocrystalline danazol in beagle dogs. *Int J Pharm* 1995;**125**:91–7.
40. Dong Y, Feng SS. Methoxy poly(ethylene glycol)-poly(lactide) (MPEG-PLA) nanoparticles for controlled delivery of anticancer drugs. *Biomaterials* 2004;**25**:2843–9.
41. Rojanasakul Y, Wang LY, Bhat M, Glover DD, Malagna CJ, Ma JKH. The transport barrier of epithelia: a comparative study on membrane permeability and charge selectivity in the rabbits. *Pharm Res* 1992;**9**:1029–34.
42. El-Shabouri MH. Positively charged nanoparticles for improving the oral bioavailabitity of cyclosporin-A. *Int J Pharm* 2002;**249**:101–8.